Inorg. Chem. **2006**, *45*, 946–948

$La_9RbIr_4O_{24}$: A Rubidium-Containing Oxide with a New Structure Type

Samuel J. Mugavero III, Mark D. Smith, and Hans-Conrad zur Loye*

Department of Chemistry and Biochemistry, University of South Carolina, Columbia, South Carolina 29208

Received November 1, 2005

Single crystals of $La_9RbIr_4O_{24}$, grown from a molten rubidium hydroxide flux, crystallize in the space group *I*4/*m* with lattice parameters $a = 7.7422(3)$ Å and $c = 17.7979(11)$ Å. The oxide forms in a new complex structure type.

The formation of oxide structures is strongly influenced by the relative sizes of the constituent cations and, in fact, for many structure types, such as rock salt, spinel, and perovskite, it is possible to anticipate their formation based on radius ratio rules.[1] Rubidium is an interesting cation in this respect because it is one of the largest in the periodic table and, curiously, rarely reported in complex oxides. Because of its large size, one would anticipate that it would be found in a high coordination number environment and, hence, not in a common structure type. In this Communication, we describe a new rubidium-containing complex oxide, $La_9RbIr_4O_{24}$, that forms in a new oxide structure type composed of layers of corner-sharing LaO_6 octahedra, IrO_6 octahedra, and RbO_{14} octa-face-capped octahedra.

Single crystals of $La_9RbIr_4O_{24}$ (Figure 1) were grown from a molten rubidium hydroxide flux. La_2O_3 (0.75 mmol), Ir metal powder (0.5 mmol), and RbOH (4.0 g) were loaded into a silver tube that had been previously flame sealed at one end. After the reactants were loaded into the tube, the other end of the tube was crimped and folded three times before being placed upright into a programmable box furnace. The tube was heated to 650 °C in 1 h, held at that temperature for 24 h, and then cooled to room temperature by shutting off the furnace. The crystals were extracted from the flux matrix by dissolving the flux in deionized water and isolating the crystals by vacuum filtration.

We have used molten hydroxide fluxes extensively to grow crystals of ternary and quaternary platinum group metal-containing oxides, where typically barium and strontium were the largest cations present. As predicted by radius ratio rules, the large size of strontium and barium relative to the smaller platinum group cations of ruthenium, osmium, and iridium often led to the growth of perovskite-type oxide crystals. Our recent experimentation with the addition of rubidium hydroxide to the hydroxide flux growth medium has resulted in the synthesis of the title compound $La_9RbIr_4O_{24}$, the composition of which was established by single-crystal X-ray diffraction. A polyhedral representation of the tetragonal structure is shown in Figure 2a and can be described as arising from the ABA′BA stacking of two different slabs: $LaRbIr_2O_{10}$ (A), and $La_8Ir_2O_{14}$ (B), where the A′ layer is offset by ($^1/_2x$, $^1/_2y$, $^1/_2z$) from the A layer. The A layer consists of a large, RbO_{14} octa-face-capped octahedron that vertex-shares with four LaO_6 octahedra at the corners of the cell and face-shares with four IrO_6 octahedra situated on the edges of the unit cell. In addition, the IrO_6 octahedra corner-share with the LaO_6 octahedra. The B layer contains five isolated IrO_6 octahedra, four of which are located on the edges of the unit cell, while the fifth octahedron is located at the center, directly below the rubidium atom of the A layer. The large size of the rubidium atom forces this central IrO_6 octahedron slightly out of the plane that contains the other isolated IrO_6 octahedra. The space in the $La_8Ir_2O_{14}$ slabs that is not occupied by the IrO_6 octahedra is filled by the lanthanum cations that are located in distorted, capped-trigonal-prismatic environments. The layers are all connected via chains of $LaO_6-IrO_6-RbO_{14}-IrO_6-LaO_6$ corner-shared polyhedra that run along the *c* direction.

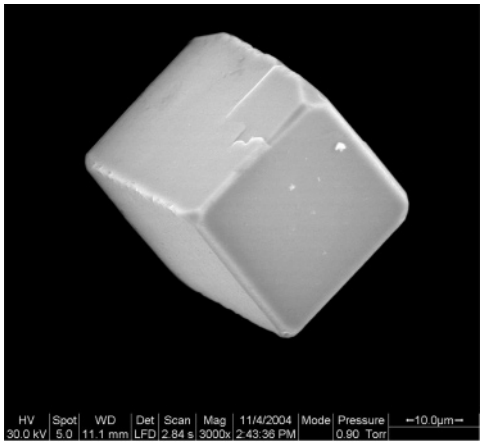

Figure 1. Scanning electron microscope picture of a single crystal of $La_9RbIr_4O_{24}$ isolated from the RbOH flux matrix.

The La−O bond distances in the LaO_6 octahedra consist of two short 2.92(13) Å bonds and four longer 2.467(9) Å bonds. The isolated IrO_6 octahedra of the A slab consist of

* To whom correspondence should be addressed. E-mail: zurloye@sc.edu. Tel: 803 777 6916. Fax: 803 777 8508.

(1) Giaquinta, D. M.; zur Loye, H.-C. *Chem. Mater.* **1994**, *6*, 365.

10.1021/ic051890s CCC: $33.50
Published on Web 01/13/2006

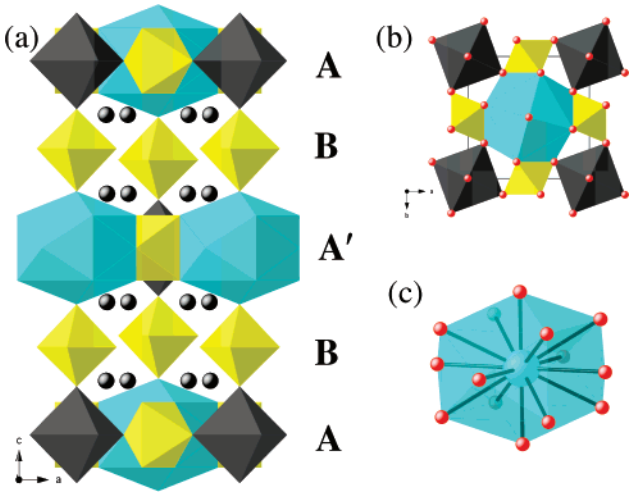

Figure 2. (a) Unit cell of $La_9RbIr_4O_{24}$ viewed down [010] (*b* axis) with Rb atoms shown in blue, Ir atoms in yellow, and La atoms black. **A** corresponds to the $LaRbIr_2O_{10}$ layer, **B** corresponds to the $La_8Ir_2O_{14}$ layer, and **A′** corresponds to the $LaRbIr_2O_{10}$ layer offset by ($^1/_2x$, $^1/_2y$, $^1/_2z$). (b) The **A** layer viewed down [001] (*c* axis). Oxygen atoms are shown as red spheres. (c) 14-fold coordination environment of the Rb atom.

two short 1.940(9) Å bonds and four longer 2.021(6) Å bonds, and the IrO_6 octahedra in the B slab consist of one short 1.938(14) Å bond, one long 1.989(13) Å bond, and four intermediate bonds of 1.958(6) Å, which are typical bond lengths found in octahedrally coordinated iridium(V)-containing oxides. The La−O bond distances in the capped-trigonal prisms range from 2.423(6) to 2.736(7) Å.

Interestingly, we can relate this new $La_9RbIr_4O_{24}$ structure type to that of the well-known perovskite structure by ignoring several of the longer Rb−O bonds, thereby limiting the coordination environment of the Rb polyhedra to that of an octahedron. The Rb−O bond distances found in the octahedra consist of four 3.267(10) Å bonds and two 2.680-(14) Å bonds, which are consistent with the bond lengths found in other rubidium-containing complex oxides.[2−5] [For the sake of this argument, we are ignoring eight only slightly longer Rb−O distances (3.319(7) Å) that would otherwise generate the octa-face-capped octahedral coordination environment.] This is depicted in Figure 3a, where the corner-sharing connectivity along the *c* direction is illustrated, now resulting from chains of LaO_6−IrO_6−RbO_6−IrO_6−LaO_6 octahedra. What makes this description so intriguing is that the A layer, shown in Figure 3b, is now reminiscent of the corner-sharing octahedral arrangement found in double perovskites. The corner-sharing of these octahedra leads to the double perovskite-type layer. Because of the very large size of the LaO_6 and RbO_6 octahedra, however, there is room for the IrO_6 octahedra, which additionally corner-share with two LaO_6 octahedra and one RbO_6 octahedron. In Figure 3b, the similarity of this layer to the layers found in double perovskites (Figure 3c) is emphasized by showing the cations in a corner-shared octahedral coordination environment.

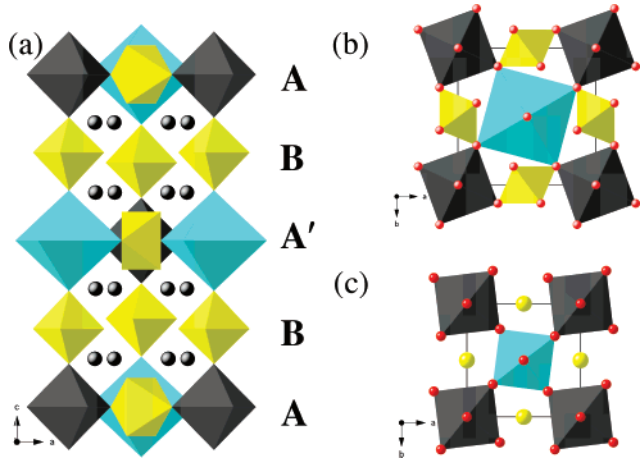

Figure 3. (a) Unit cell of $La_9RbIr_4O_{24}$ viewed down [010] (*b* axis) with Rb atoms shown as blue octahedra. (b) The **A** layer viewed down [001] (*c* axis) shown as it is related to the double perovskite structure. Notice that the IrO_6 octahedra (yellow) are no longer face-shared to the Rb polyhedra. (c) Corner-sharing connectivity of a generic, tilted, $A_2BB'O_6$ double perovskite that is related to the connectivity of $La_9RbIr_4O_{24}$ shown above.

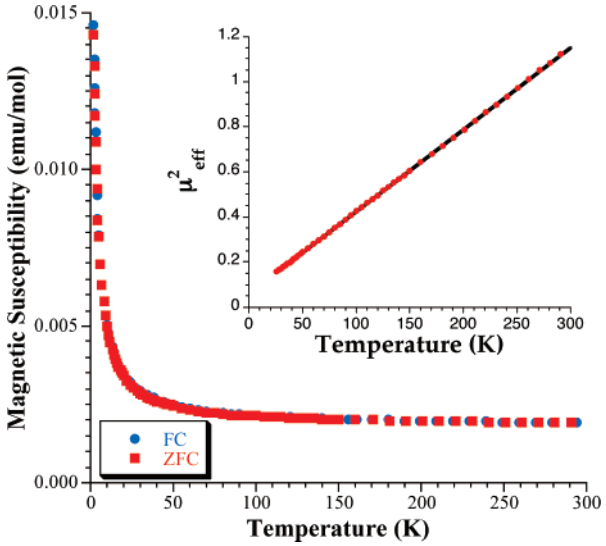

Figure 4. Temperature dependence of the ZFC (squares) and FC (circles) magnetic susceptibility of $La_9RbIr_4O_{24}$. Inset: Temperature dependence of the squared magnetic moment of $La_9RbIr_4O_{24}$. A linear fit of the data is shown as a solid line.

Notice how the IrO_6 octahedra of the B slab trans-vertex-share oxygens with the LaO_6 and RbO_6 octahedra and how this LaO_6−IrO_6−RbO_6−IrO_6−LaO_6 linkage prevents corner sharing between the IrO_6 octahedra in the B slabs. The much larger size of the LaO_6 and RbO_6 octahedra causes the iridium cations to be separated from one another sufficiently to prevent corner sharing.

The temperature dependence of the magnetic susceptibility for $La_9RbIr_4O_{24}$ is shown in Figure 4. The susceptibility increases with decreasing temperature over the entire measured temperature range, and the zero-field-cooled (ZFC) and field-cooled (FC) data overlay in all cases.

It is known that iridium(V) has a nonmagnetic ground state and therefore contributes very little to the overall susceptibility.[6−11] Furthermore, because of the fact that in this structure the iridium cations are all isolated, we do not expect significant magnetic coupling between them. We can deter-

(2) Armstrong, R. A.; Anderson, P. A. *Inorg. Chem.* **1994**, *33*, 4366.
(3) Kumada, N.; Iwase, E.; Kinomura, N. *Mater. Res. Bull.* **1998**, *33*, 1729.
(4) Toda, K.; Sato, M. *J. Mater. Chem.* **1996**, *6*, 1067.
(5) Porter, Y.; Halasyamani, P. S. *J. Solid State Chem.* **2003**, *174*, 441.

mine the magnetization at zero temperature following the procedure of Hayashi et al., which was later modified by Darriet et al., by plotting the squared magnetic moment as a function of temperature.[8,11] From a linear fit extrapolation of this plot to zero temperature, it is possible to calculate the iridium(IV) content in this compound that could arise from an oxygen deficiency. The μ^2 vs T plot, shown as the inset in Figure 4, corresponds to an iridium(IV) (d^5, $s = {}^1/_2$) content of no more than 2.0%.

ζ crystal data: X-ray intensity data of a small black-block crystal were measured at 150(1) K on a Bruker SMART APEX CCD-based diffractometer system using Mo Kα radiation ($\lambda = 0.710\,73$ Å). $La_9RbIr_4O_{24}$, $M = 2488.46$ g mol^{-1}, tetragonal, space group $I4/m$ (No. 87), $a = 7.7422(3)$ Å, $c = 17.7979(11)$ Å, $V = 1066.84(9)$ Å^3, $Z = 2$, $D_c = 7.747$ Mg m^{-3}, μ(Mo Kα) = 44.783 mm^{-1}, crystal size 0.04 × 0.04 × 0.02 mm^3, θ range 2.29−30.50°, 9959 reflections collected, 843 independent ($R_{int} = 0.0442$), data/restraints/parameters 843/0/46, R1(F) = 0.0300, wR2(F^2) = 0.0652, GOF = 1.098 (all data), ρ(max/min) = +2.31/−3.75 e Å^{-3}. The structure was solved and refined using SHELXTL version 6.1. ICSD reference number 415532. ξ magnetism: Magnetic susceptibility measurements were performed on loose crystals of $La_9RbIr_4O_{24}$ using a QD MPMS XL SQUID magnetometer. The sample was measured under both ZFC and FC conditions in applied fields of 10 kG over the temperature range of 2 K ≤ T ≤ 300 K. The sample was contained in a gel capsule suspended in a plastic straw for immersion into the SQUID.

Acknowledgment. Financial support for this research was provided by the Department of Energy through Grant DE-FG02-04ER46122 and the National Science Foundation through Grant DMR-0450103.

Supporting Information Available: CIF files for $La_9RbIr_4O_{24}$. This material is available free of charge via the Internet at http://pubs.acs.org.

IC051890S

(6) Powell, A. V.; Gore, J. G.; Battle, P. D. *J. Alloys Compd.* **1993**, *201*, 73.
(7) Walewski, M.; Buffat, B.; Demazeau, G.; Wagner, F.; Hagenmuller, P. *Mater. Res. Bull.* **1983**, *18*, 881.
(8) Hayashi, K.; Demazeau, G.; Pouchard, M.; Hagenmuller, P. *Mater. Res. Bull.* **1980**, *15*, 461.
(9) Davis, M. J.; Mugavero, S. J., III; Glab, K. I.; Smith, M. D.; zur Loye, H.-C. *Solid State Sci.* **2004**, *6*, 413.
(10) Wakeshima, M.; Harada, D.; Hinatsu, Y. *J. Alloys Compd.* **1999**, *287*, 130.
(11) Darriet, J.; Demazeau, G.; Pouchard, M. *Mater. Res. Bull.* **1981**, *16*, 1013.